frontiers in Earth Science

ORIGINAL RESEARCH
published: 28 March 2022
doi: 10.3389/feart.2022.827438

Multi-Hazard Chain Reaction Initiated by the 2020 Meilong Debris Flow in the Dadu River, Southwest China

Lan Ning[1,2,3], *Kaiheng Hu*[1,2]*, *Zhang Wang*[1,2,3], *Hong Luo*[4], *Haokun Qin*[5], *Xiaopeng Zhang*[1,2,3] *and Shuang Liu*[1,2]

[1]Key Laboratory of Mountain Hazards and Earth Surface Processes, Chinese Academy of Sciences, Chengdu, China, [2]Institute of Mountain Hazards and Environment, Chinese Academy of Sciences, Chengdu, China, [3]University of Chinese Academy of Sciences, Beijing, China, [4]Sichuan Institute of Land and Space Ecological Restoration and Geological Hazard Prevention, Chengdu, China, [5]Sichuan Metallurgical Geological Survey Bureau, Chengdu, China

Delivery of large volumes of sediment by debris flows in a short time into rivers often initiates a hazardous chain reaction in alpine valleys. Predicting the multi-hazard chain's evolution and intervening in its cascading effects by artificial countermeasures face major challenges due to the spatial and temporal variability of controlling factors. On June 17, 2020, a rainstorm-induced debris flow event with a volume of 2.4×10^5 m^3 occurred in the Meilong catchment, Danba County, Sichuan Province, Southwest China, which triggered a debris flow–outburst flood–landslide hazard chain. Large amounts of sediment entered the Xiaojinchuan River and formed a barrier lake. The outburst flood and narrowed river flow eroded 2.76×10^6 m^3 of deposits and reactivated the Aniangzhai landslide. Engineering measures were implemented to prevent the hazard, including dredging, rechanneling, and embankment construction. The deformation rate and acceleration of the landslide decreased from a peak of 75 mm/h to 8.74 mm/h and a peak of 16.46 mm/h^2 to 0.13 mm/h^2 before and after the engineering, respectively, according to measurements of a ground-based monitoring radar. Without the engineering measures, the factor of safety of the landslide would be reduced to 0.93, and a larger landslide dam hazard would occur if the foot were eroded by more than 17 m. The case and its successful engineering demonstrate that artificial intervention measures are effective in halting the cascading process of natural hazards.

Keywords: debris flow, cascading hazards, landslide stability, barrier lake, river erosion

OPEN ACCESS

Edited by:
Jean-Claude Thouret, Clermont Université, France

Reviewed by:
Jonathan Procter, Massey University, New Zealand
Vern Manville, University of Leeds, United Kingdom

***Correspondence:**
Kaiheng Hu
khhu@imde.ac.cn

Specialty section:
This article was submitted to Geohazards and Georisks, a section of the journal Frontiers in Earth Science

Received: *02 December 2021*
Accepted: *15 February 2022*
Published: *28 March 2022*

Citation:
Ning L, Hu K, Wang Z, Luo H, Qin H, Zhang X and Liu S (2022) Multi-Hazard Chain Reaction Initiated by the 2020 Meilong Debris Flow in the Dadu River, Southwest China. Front. Earth Sci. 10:827438. doi: 10.3389/feart.2022.827438

INTRODUCTION

Large debris flows or avalanches that occur in narrow alpine valleys are likely to block rivers and trigger a multi-hazard chain, causing serious damage to settlements and infrastructure (Davies 1997; Korup and Clague 2009; Cui et al., 2015). The chain usually comprises landslides, dammed lakes, and outburst floods (Reneau and Dethier 1996; Cui et al., 2011; Kappes et al., 2012). In general, the total loss caused by such a multi-hazard chain is far greater than that caused by a single hazard (Chai et al., 1995; Xu et al., 2010; Chen et al., 2011; Ma and Kaiheng, 2013). Recent events, e.g., the 2007 and 2010 Tianmo debris flows (Ge et al., 2014; Deng et al., 2017) and the 2018 Sedongpu debris flows in southeastern Tibet (Hu K. et al., 2019), demonstrate that the multi-hazard chain may affect great spatial and temporal extents than a debris flow.

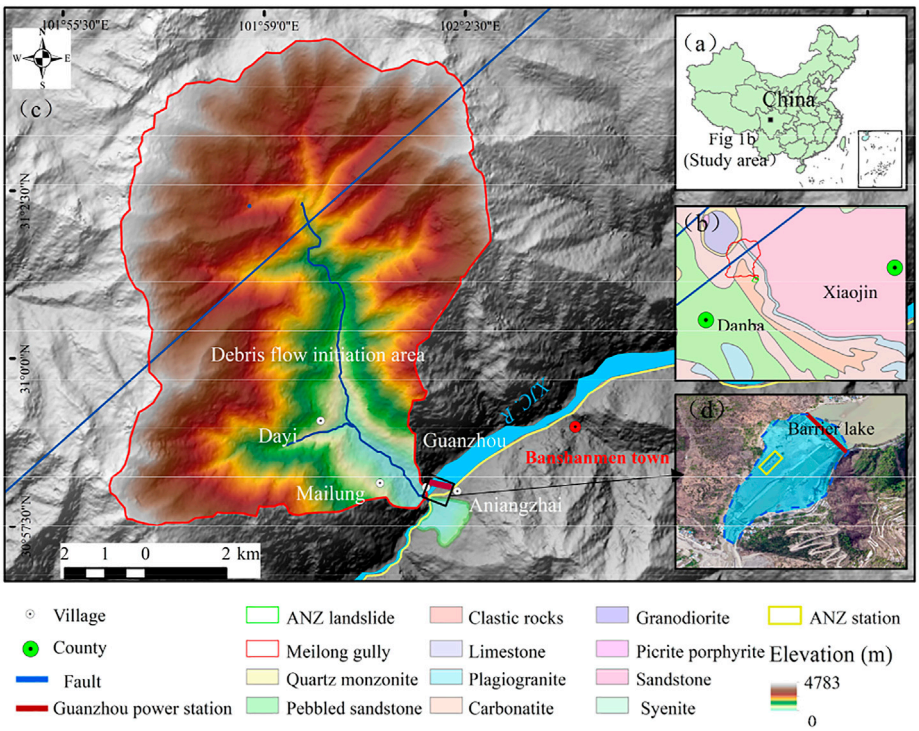

FIGURE 1 | Regional settings and locations of the Meilong valley and ancient ANZ landslide. **(A)** Location of the study area. **(B)** Lithology of the study area. **(C)** Topographic features and fault distribution. **(D)** Meilong barrier lake. XJC R is the Xiaojinchuan River. ANZ L is the Aniangzhai landslide.

Previous researches are focused on the transformation mechanism, theoretical description, numerical simulation of multi-hazard chains, and decision-making. Papathoma-Köhle et al. (2011) analyzed medium-scale multi-hazards by considering disposition alteration and hazard linkage. van Westen et al. (2014) performed a quantitative hazard risk assessment of gravitational processes, including landslides, debris flows, rockfalls, snow avalanches, and floods, in the Barcelonnette area, French Alps. Worni et al. (2014) proposed an integrated method of modeling a typical process of glacial lake outburst floods by combining numerical models of impulse wave, dam breaching, and flood propagation. Chen et al. (2016) implemented a quantitative model of hazard risk assessment integrated with expert opinion in a valley prone to debris flows and floods in the northeastern Italian Alps. Liu and He (2018) simulated a rockslide-triggered multi-hazard chain by using a finite volume method. Recently, a comprehensive method was developed for quantitatively evaluating the risk of a potential debris flow multi-hazard chain (Hu et al., 2018; Hu K. et al., 2019; Hu X. et al., 2019; Luo et al., 2020). Efforts of engineering measures have been made to prevent and control multi-hazard chains, such as those caused by the 2008 Wenchuan earthquake (Xu et al., 2012). The chains are characterized by the so-called cascading effect or domino effect (Delmonaco et al., 2006; Carpignano et al., 2009), i.e., a natural hazard triggers one or more hazards, and the risk spreads over a more extensive space and longer time period. Kappes et al. (2012) pointed out that the interaction among hazards often results in risk amplification, and the means for considering the cascading effects in reducing risk remains a huge challenge.

On June 17, 2020, a rainstorm-induced debris flow event with a volume of 2.4×10^5 m^3 occurred in the Meilong basin, Danba County of Sichuan Province, Southwest China (**Figure 1**). Approximately 1.3×10^5 m^3 of sediment was deposited in the Xiaojinchuan River (XJC), a tributary of the Dadu River, and partially blocked the river channel. Debris-flow deposition forced the river course to move to the left bank, and then the rapid flow strongly eroded the foot of the old Aniangzhai (ANZ) landslide, leading to the reactivation of the 6.2×10^6 m^3 landslide. It is a typical debris flow–outburst flood–landslide chain with intense cascading effects. To stop the chain from developing into a large dammed lake and subsequent catastrophic outburst flood, the government cleared the sediment and recovered the river path. The engineering measures effectively prevented the landslide and eliminated the risk of dammed lake. In this paper, we describe the evolving process of the multi-hazard chain and quantitatively evaluate the cascading consequences with and without controlling measures.

STUDY AREA

The event occurred in Banshanmen town, Danba County, western Sichuan Province, China (**Figure 1A**). It is part of the

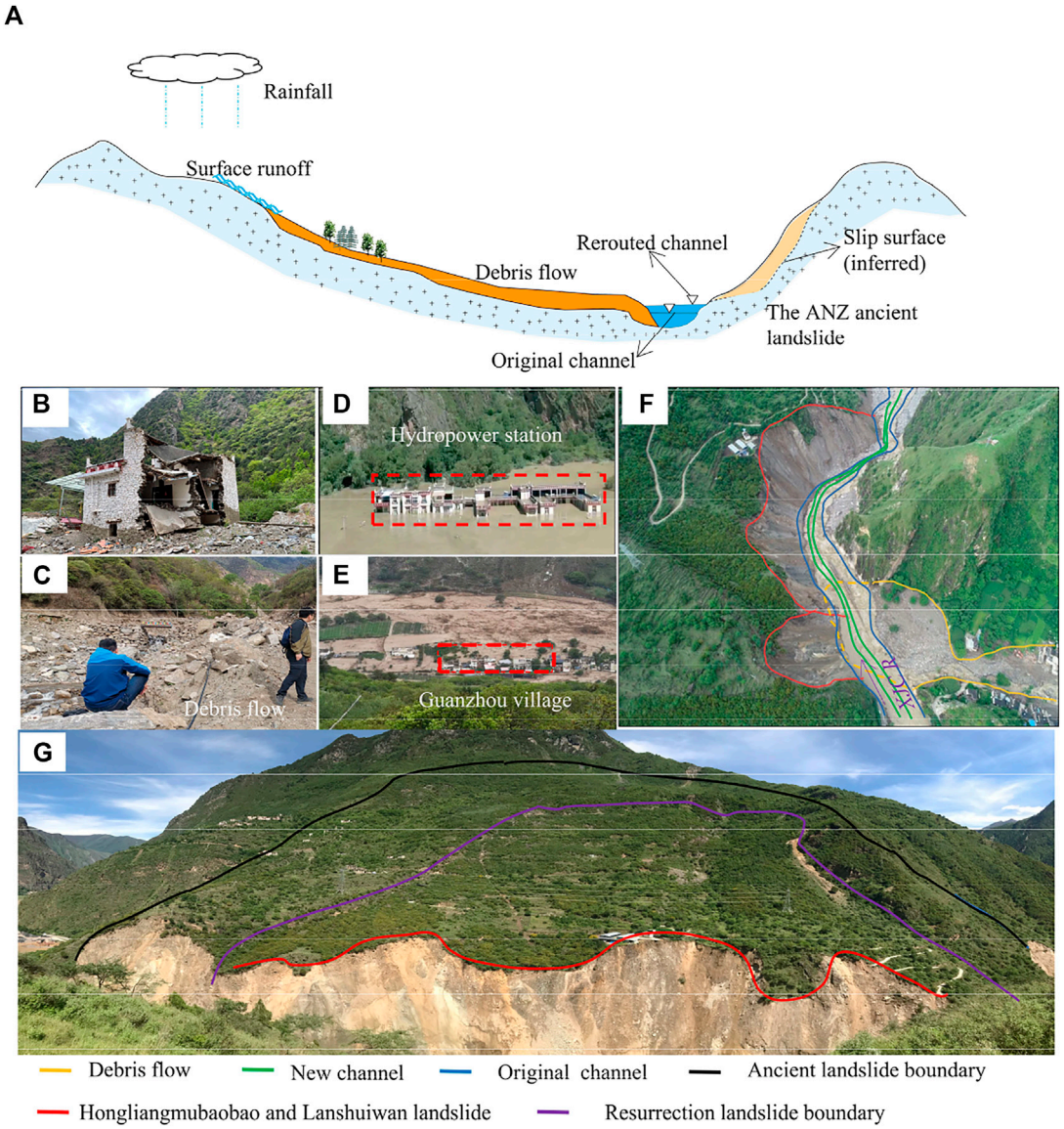

FIGURE 2 | Multi-hazard chain caused by the Meilong debris flow. (b–g) On-spot photos and unmanned aerial vehicle (UAV) images taken in the field survey. **(A)** Schematic of the multi-hazard process; **(B,C)** houses destroyed by the debris flow and debris-flow deposits in the Meilong channel; **(D,E)** the dammed lake and Guanzhou village damaged by the flood; **(F,G)** the ancient ANZ landslide.

transition zone between the Qinghai-Tibetan Plateau and the Sichuan Basin and is part of the alpine valley area with high denudation. The tectonic units of Danba belong to the Songpan-Garze fold system, which is the southern part of the Bayankala Mountains, and the Songpan-Garze fold system is surrounded by the Xianshuihe fault belt, the Longmenshan fault belt, and the South Qinling fault belt. The terrain is generally high in the south and low in the north (Sun and Li 2019). The lithology is complicated and dominated by granite and psammite (**Figure 1B**).

The Meilong basin (**Figure 1C**) is on the right bank of the XJC, a major tributary of the Dadu River. It has a catchment area of 63.2 km^2, and the elevation between 2,125 to 4,783 m. The mainstream channel is 10.2 km long and 30 ~ 60 m wide, with a gradient of 253‰ and bank slope of more than 40°. A debris flow occurred in 1952 (Zhao et al., 2021), and about 84.8×10^5 m^3 (data from the Danba County Water Resources Bureau) of loose material is stored in the basin as supplies to debris flows.

The climate is affected by the Indian monsoon, which causes precipitation of 617 mm per year. According to the rainfall data of the Danba meteorological station over the past 33 years, the rainy season extends from May to September with a total rainfall of more than 460 mm, about 73.3% of the annual rainfall. The daily precipitation is large in July and August, and the maximum

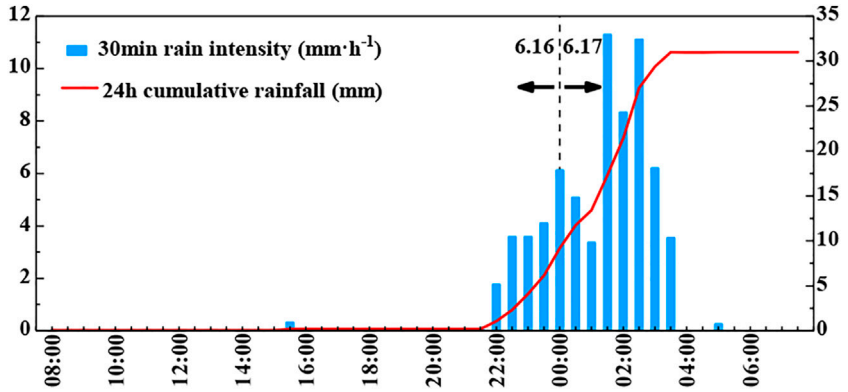

FIGURE 3 | Curve of rainfall at Banshanmen town, Danba County, on June 16 and 17, 2020.

monthly rainfall occurs in September, on average of 109.12 mm (Sun and Li 2019). The rainfall is in short duration and high concentration. From June 8 to 17, 2020, the study area experienced continuous rainfall of 271.6 mm, 1.1 times higher than the historical record since 1951.

"JUNE 17" MEILONG DEBRIS FLOW AND SUBSEQUENT CASCADING HAZARDS

The hazard was a combination of a debris flow, barrier lake (partially damming), outburst flood, and landslide (**Figure 2A**). On June 17, 2020, a debris flow first occurred upstream of Dayi gully (blue dots in **Figure 1C**), a left tributary of the Meilong basin. The flow then entered the XJC and accumulated at the confluence and partially dammed the river to form an ephemeral lake (**Figure 2D**). Two hours later, the dam failed, and the lake outburst increased the river discharge, which changed the river channel. The rerouted channel caused the outburst flood to erode the foot of the ANZ, inducing two small landslides (**Figure 2F**). The loss of mass at the foot and the continuous erosion of the river reactivated the ANZ landslide (**Figure 2G**).

Meilong Debris Flow

The intense rainfall-triggered debris flow initiated at the Dayi gully and ended in the XJC (**Figure 3**). According to the local meteorological bureau, the sudden rainfall started at 23:40 on June 16, 2020. The GPM rainfall data based on satellite remote sensing inversion show that the rainfall intensity reached a maximum of 11.28 mm/h about 2 h before the debris flow. The rainfall intensity was as high as 11.10 mm/h 1 h before the occurrence, and the accumulated rainfall was 30 mm when the debris flow occurred (**Figure 3**). Sediment was quickly eroded along the flow path, and the main area of erosion is a Quaternary accumulation terrace near the Dayi gully (**Figure 1**). The debris flow lasted for approximately 40 min with a peak velocity of 8.2 m^3/s (Zhao et al., 2021), transporting 2.4×10^5 m^3 of material and forming a 3.0×10^4 m^2 deposit fan. Approximately 1.3×10^5 m^3 of sediment was transported into the main river, and the fan was approximately 1.1×10^5 m^3 (Hu et al., 2020). According to the field investigation, the flow is 20–80 m wide and 3 m in depth, with boulders ranging between 0.1 and 0.5 m in diameter, up to the maximum of 5 m (**Figure 2C**). Several houses were buried and damaged by the debris flow (**Figure 2B**).

Barrier Lake and Outburst Flood

The debris flow and subsequent small landslides deposited large amounts of sediment in the XJC, forming a barrier lake of 200 m long, 50 to 100 m wide, and 8 to 12 m high. According to remote sensing images, the maximum area of the lake was 1.45×10^5 m^2 (**Figure 1D**), and the submerged area was 1.13×10^5 m^2. The surface was 4.6 m higher than the river and flooded the first floor of the ANZ station (**Figure 1D**). The volume of the lake was 6.62×10^5 m^3. Threatened by such a dam that is usually unstable and has a shorter life (Fan et al., 2020), more than 21,200 people in the downstream towns were evacuated. The barrier lake completely breached only about 2 h later, and the flooding process began at 12 p.m. and ended at 4 p.m. The discharge of the outburst flood is 492 m^3/s, the same order of magnitude as the seasonal flood flow, but the dam moved the river channel 20 m to the left. The flood damaged No. 303 provincial road (S303 in **Figure 4**) on the left bank and seriously eroded the foot of the ANZ. In addition, many houses, a large area of farmland, and about 20 km of roads were flooded downstream, and the flooded area of Aniangzhai village was approximately 0.8 km^2. The outburst flood induced six landslides, among which the largest landslide was the ANZ (Yao et al., 2020).

Reactivation of the ANZ Landslide

The ANZ is a bedrock landslide with an area of 1.4 km^2 and a thickness of 50 m. It occurred 120 years ago and blocked the river. In recent years, the landslide has crept slowly, with occasional cracks appearing in buildings and farmland on the landslide. Satellite images also showed some small-scale historic landslides. Nonetheless, the ANZ remains stable on the whole. However, the outburst flood erosion of the slope foot has caused two small landslides, the Hongliangmubaobao landslide and

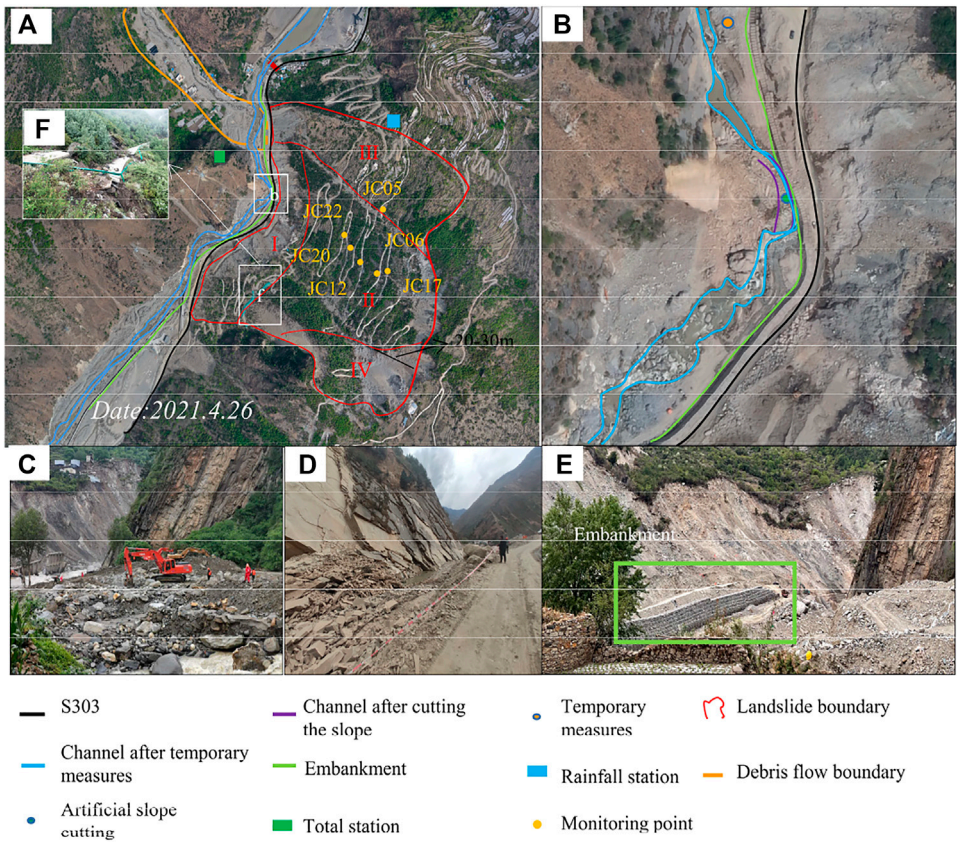

FIGURE 4 | Changes in the Meilong valley around the ANZ landslide and engineering measures after the debris-flow event. **(A)** Detailed characteristics of the reactivated ANZ area and emergency monitoring scheme. (I: front collapse zone, II: main deformation zone, III: upstream deformation zone, IV: downstream deformation zone). **(B)** Influence of engineering measures on channel evolution. **(C)** Temporary engineering measures: the excavator dredging the river. **(D)** Workers blasting the slope. **(E)** Temporary embankment. **(F)** Road falling apart.

Lanshuiwan landslide, which formed a free face about 60 m high. The instability of the foot and the continuous erosion of the river induced the ANZ to reactivate and slide.

RIVER EROSION AND LANDSLIDE DEFORMATION

Sediment usually forms dams and blocks rivers after landslides or debris flows (Costa and Schuster 1988; Hermanns et al., 2004). If the dam breaks, the outburst flood can cause serious harm downstream (Fan et al., 2012). Dams can be divided into complete dams and partial dams depending on the volume and composition of debris flows, which cause different changes in river morphology. If the riverbank is part of the diversion channel, the narrowing flow accelerates the bank erosion (Costa and Schuster 1988; Abidin et al., 2017). The Meilong debris flow formed a partial dam. After the dam broke, the flood altered the position of the channel and intensified the erosion on the left bank, leading to landslide reactivation.

The Lanshuiwan and Hongliangmubaobao landslides in front of the ANZ have moved 3–15 m with a volume of 2.76×10^6 m^3 entering the channel (**Figure 2F**). There was obvious deformation at the back and some cracks in the middle (**Figure 3G**). The road on the landslide was destroyed with a vertical dislocation of 5–14 m (**Figure 4F**). The horizontal and vertical displacement at the foot are 15–20 m and 15–25 m, respectively; and a large number of fractures formed near the downstream boundary. The displacement at the back of the landslide reached 20–30 m (**Figure 4A**), an increase of 5–10 m compared to August 20, 2020. A new channel is cut at the foot of the landslide, and the current channel becomes wider than ever (**Figure 2F**). Now the government has carried out engineering measures, including dredging (**Figure 4C**), changing the channel position (**Figure 4B**, **Figure 3D**), and building embankments (**Figure 4E**).

A ground-based radar for emergency monitoring detected the accelerating deformation of the landslide from June 18 to August 20, 2020. Rainfall and river discharge were monitored to investigate the landslide variability. Monitoring points 2, 23, 20, and 9 were set up in front collapse zone I, main deformation zone II, upstream deformation zone III, and

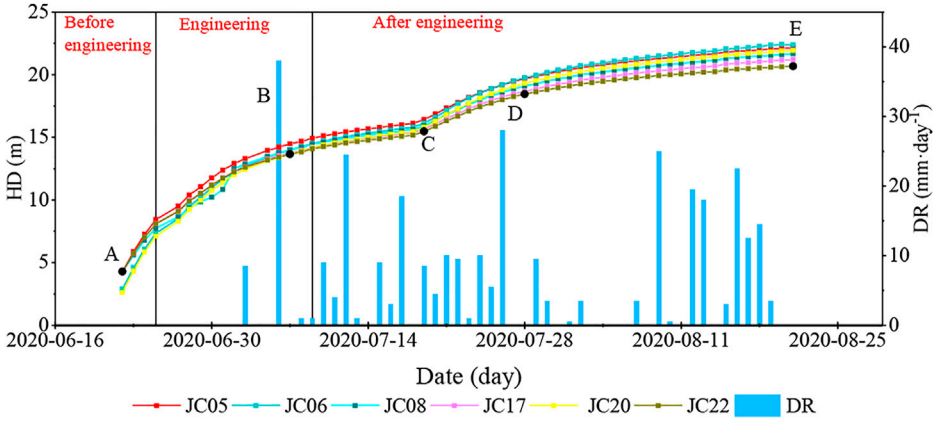

FIGURE 5 | Landslide cumulative surface displacement and monitoring daily rainfall (DR: daily rainfall; HD: horizontal displacement).

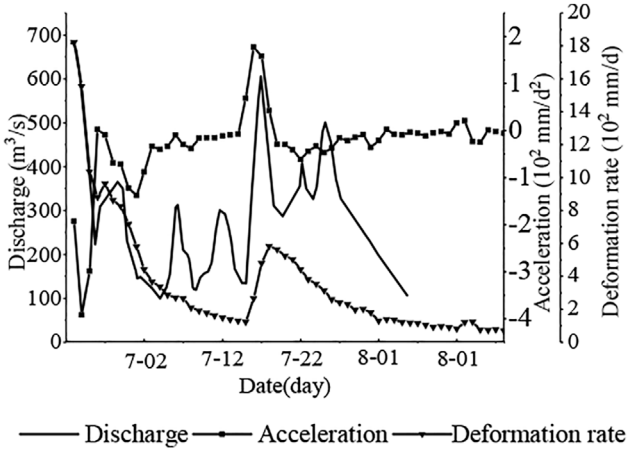

FIGURE 6 | Deformation rate and acceleration of monitoring point JC22 and river discharge. The river flow data are from the Guanzhou power station, whose location is shown in **Figure 1D**. The river flow data in **Figure 6** are the same as those in **Figure 7**.

downstream deformation zone IV, respectively. Six representative points were selected to represent the deformation of the landslide (**Figure 4A**). We find that landslide displacement is greatly affected by river discharge and engineering (**Figure 5**). The maximum and minimum velocity and acceleration of the landslide motion ranged from 75 mm/h and 16.46 mm/h^2 to 8.74 mm/h and 0.13 mm/h^2, respectively, before and after engineering measures (**Figure 6**). Moreover, the coupling of rainfall and fissures within the ANZ landslide accelerates the displacement rate, which is consistent with the new development of fissures in its back (**Figure 4A**). The ANZ landslide experienced four stages: two rapid displacements (A-B and C-D) and two slow displacements (B-C and D-E). After the dam failed, the outburst flood eroded the foot of the landslide, resulting in the rapid displacement (A-B), with a sliding distance of 12 m in 10 days. As the river moved away from the foot (B-C), the displacement gradually slowed down to 3 m in 15 days. A change in the water level reduced the pore water pressure of the soil beneath the landslide and caused the stress redistribution of the whole slope (Rahardjo et al., 2001). The dissipation process of pore water pressure resulted in changes in soil strength and accelerated the displacement of the landslide, which was 4 m in 8 days (C-D). The deformation rate of the landslide controls the development of excess pore water pressure, and the excess pore water pressure determines the change in shear strength of the soil. When the reduced sliding resistance is less than the sliding force, the landslide slides, and then the landslide reaches a new stress equilibrium. The process is controlled by the dissipation of pore water pressure, which lags behind the change in the channel position, and in this case, it lagged 15 days. Then, the landslide entered the slow displacement stage (D-E) again, with a displacement of 4 m in 26 days. As shown by the displacement curve, the channel position directly affects the stability of the landslide but lags behind the change in river position.

In this study, we refer to the seepage monitoring model to consider the hysteresis effect.

$$v = v_0 + \frac{\tau - \tau_f}{m} t = v_0 + \frac{\tau - \left\{c' + \left[\sigma - \left(u_w + p\left(Z, t_{diff}\right)\right)\tan\phi'\right]\right\}}{m} t$$

where v is the velocity of the landslide (m/s); v_0 is the initial velocity of the landslide; τ is the shear sliding force acting on the sliding surface (kPa); τ_f is the resistance along the sliding surface (kPa); t is time (s); σ is the total stress (kPa); c is the cohesive force (kPa); ψ is the internal friction angle (°); u_w is the pore water pressure (kPa); c' is the effective cohesion (kPa); ψ' is the effective internal friction angle (°); and p (z, t) is the pore water pressure increment at time t and depth z of the sliding block (kPa).

Therefore, under the limit equilibrium state, the rise and fall of pore water pressure on the sliding surface will lead to the acceleration $(V > 0)$ or deceleration $(V < 0)$ of land sliding.

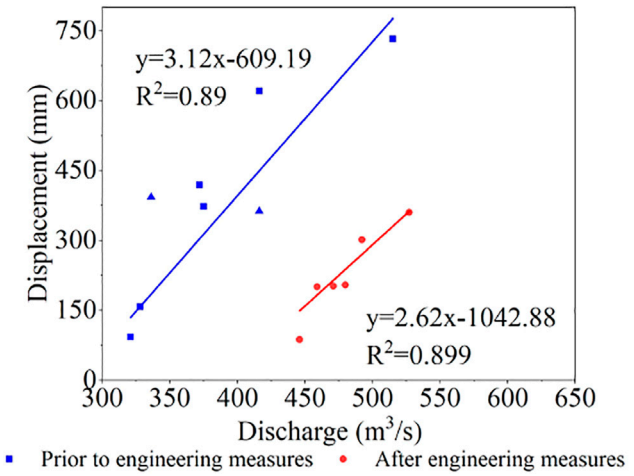

FIGURE 7 | Relationship between river discharge and horizontal displacement of the landslide before and after the engineering measures were implemented. Triangle data are from Zhao et al. (2021).

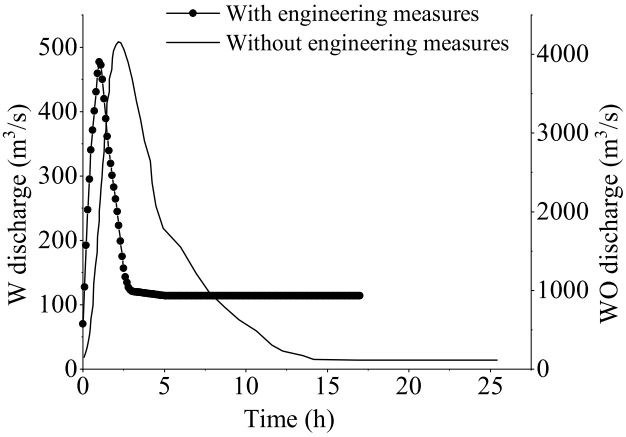

FIGURE 8 | Discharge hydrograph of the outburst floods with and without engineering measures (W: with engineering measures, WO: without engineering measures).

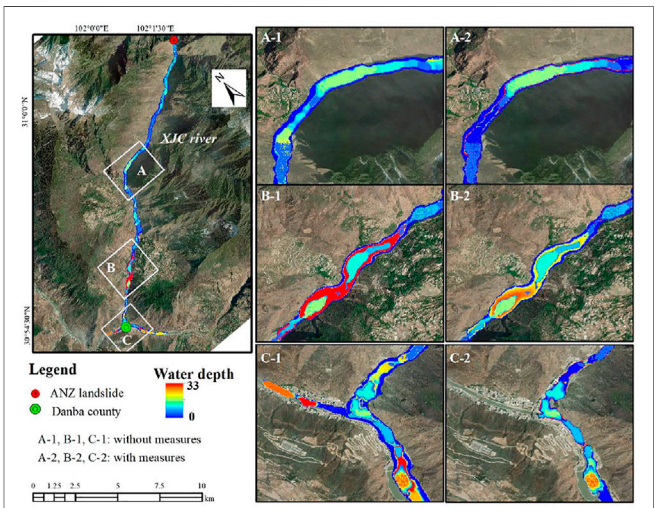

FIGURE 9 | Spatial distribution of the computed maximum flow depth. A-1, B-1, C-1: without engineering measures, A-2, B-2, C-2: with engineering measures.

When the river flow increases, the pore pressure rises, so the landslide movement accelerates (**Figure 6**). However, the pore water pressure increment generated by rainfall and river flow changes needs time to act at the sliding surface. This lag time t_{diff} is closely related to the hydraulic diffusion coefficient and the landslide thickness. Thus, it indicates that the landslide displacement lags behind the change in river discharge (**Figure 5**).

To describe the influence of channel position on the landslide stability, we draw a scatter plot according to the relationship between river discharge and landslide displacement in the two stages (**Figure 7**), which shows a good linear relationship; and the influence of river discharge on landslide stability has been greatly decreased by engineering measures. Two straight lines ($y = Ax + B$) were obtained by fitting the scattered points, where A represents the ability of discharge to influence the landslide displacement, and B/A represents the minimum discharge required to generate displacement. Before the engineering measures were implemented, landslide displacement occurred when the river flow was 126.76 m^3/s (the blue line in **Figure 6**), but the threshold for displacement increased to 398.05 m^3/s (the red line in **Figure 6**) after the engineering measures were implemented. The ability of river flow to affect the landslide before the engineering measures were implemented was 1.19 times (the ratio of the blue line's slope to the red line's slope in **Figure 6**) that after the engineering measures were implemented.

The fluvial erosion due to the river channel change has the greatest influence on the stability of the landslide. Therefore, the most significant impact of the engineering measures is to change the position of the channel, which prevents erosion at the foot of the landslide, thereby preventing a reduction in slide resistance. The change in the channel position also reduces the ability of discharge to affect landslides.

HAZARD ASSESSMENT WITH AND WITHOUT THE ENGINEERING MEASURES

Engineering measures lowered the risk or probability of the hazard reoccurring. To directly represent the impact of engineering measures, we calculated the flow duration curve without engineering measures and the hazard assessment before and after engineering measures (**Figures 8**, **9**).

The total volume of the ancient ANZ landslide is estimated as 6×10^6 m^3, which would form a dam at least 100 m high and impound water of 8.2×10^8 m^3. Chen et al. (2015) proposed the hyperbolic model of soil erosion rate and the circular sliding surface method with the lateral expansion of the gap. The governing equations are solved using a

numerical method that allows simple calculations in Excel 2007 spreadsheets. Using the DB-IWHR dam flood analysis program, the maximum flow at the barrier dam without engineering measures was 4,180 m^3/s (10 times as much as after engineering measures were taken), and then the flow gradually decreased. Approximately 6 h after the outburst, the flow attenuated to 1,536 m^3/s, attenuating by approximately 63.1%; approximately 11 h after the outburst, the flow attenuated to 413 m^3/s, attenuating by approximately 89.7% (**Figure 8**).

With the two discharge hydrographs corresponding to natural evolution and engineering intervention, a computational program developed by Ouyang et al. (2013) is applied to simulate the propagation of the outburst floods. The governing equation of flood movement is the diffusion wave equation obtained by simplifying the depth integral of Navier-Stokes equation and ignoring the convective term of momentum equation, and then solved by a first-order upwind finite difference scheme. The basal friction relationship is the traditional Manning's model. The flood hazard is related to destructive power of a flood such as flow depth, velocity, or impact force. We use the maximum flow depth as the proxy of the flood hazard (**Figure 9**). The flood will reach the city of Danba after passing the confluence of Dajinchuan and XJC rivers and move upstream along the Dajinchuan River if without engineering measures. The inundation area of the city will be approximately 130,000 m^2 and the maximum runoff depth reaches 33 m (**Figure 9**-C-1). The area with the maximum flow depth >10 m accounts for 16.19% of the total area. However, due to the timely engineering measures implemented by the government, the dam-break flood propagated downstream of the Dadu River and did not reach the Danba city upstream (**Figure 9**-C-2). The area with the maximum flow depth >10 m only accounts for 6.79% of the total area, a reduction of 9.4% compared with no engineering measures.

DISCUSSION

Previous studies on multi-hazard chain have emphasized the role of engineering measures (Gilbuena Jr et al., 2013; Bouwer et al., 2014). Mechler (2016) apply CBA (CBA is a major decision-supporting tool used by governments to organize and calculate the societal costs and benefits) to hazard risk reduction (DRR), which believes that the short-term method to break the hazard chain is mainly using engineering measures. On October 10, 2018, a landslide hazard chain occurred at Baige, Jiangda County, Tibet, China on the Jinsha River. In the Baige multi-hazard chain, the Chinese government decided to dig a spillway 33 m deep and 10.89 m wide at the bottom and 120.57 m wide at the top. The spillway was completed 2 days before the breaching of the dam. Later, this was shown to be extremely effective (Zhang et al., 2020). The Hongshiyan landslide dam formed by the 2014 Ludian earthquake in Yunnan Province, China also adopted a similar mitigation measure as the Baige landslide hazard chain (Shi et al., 2017). Similar to previous studies, the Chinese government also took engineering measures to change the channel position and thus truncate the Meilong multi-hazard chain.

The influence of channel position on landslide deformation is important. In this paper, the main factor affecting the stability of the ANZ landslide is the erosion of the slope foot by flood. Therefore, to quantify the influence of flood erosion on the stability of ANZ landslide, Janbu method was adopted to calculate the stability of landslide. The Janbu method assumes that the force is applied to one-third of the height of the block, and each block satisfies both static equilibrium conditions and limits equilibrium conditions. The slip zone also satisfies the torque equilibrium condition.

The stability factor of the ANZ after engineering was 1.09 by assuming that $\gamma = 20$ kN/m^3, $\varphi = 20^{\circ}$, and $c = 19$ kPa (Yu, 2018). If the river continues to erode horizontally to 17 m, the stability factor would drop to 0.93, and the landslide would slide down. When we returned in April 2021, the landslide had not slid down as a whole and was stable. Therefore, we can express that the government's engineering measures delayed and reduced the acceleration of landslide deformation, stopped the multi-hazard chain, and protected the safety of downstream residents, especially Aniangzhai village to Danba County along the XJC River.

CONCLUSION

On June 17, 2020, the Meilong debris flow triggered a multi-hazard chain, including the formation of a dammed lake, a subsequent outburst flood, and reactivation of the ANZ by toe erosion. Without intervention, the landslide could trigger a larger multi-hazard chain, threatening the downstream area. Therefore, the government implemented timely engineering measures. By analyzing the blocking effect of engineering measures and quantitatively evaluating the cascading consequences of the multi-hazard chain with and without artificial intervention measures, we draw some conclusions.

The landslide had a large displacement before the engineering measures were implemented; and the measures have changed the river channel 20 m away from the slope foot and prevented the slope erosion. The change in the channel position also led to the gradual decrease in pore water pressure and the decrease in total stress at the foot of the slope, resulting in the redistribution of stress and a short rapid displacement of the landslide. This phenomenon lagged behind the change in the channel position due to the slow dissipation of pore water pressure. That is, in the first stage, the water level of the river inundated the slope foot. This means lateral support of flooding water while there is severe erosion at the same time. If this river support is withdrawn by displacement of the river and the water level drops, the seepage pressure of the dissipating water at the foot will at first decrease the stability at the foot and hence the stability of the entire landslide. However, drainage at the foot also means a

drawdown of the water table all over the landslide and an increase in instability.

We calculated the stability of the landslide by the Janbu method. The safety factor of the ANZ is currently 1.09, but it will drop to 0.93 if the river continues to erode the foot of the landslide by 17 m. Without engineering measures, a 100m-high dammed lake with a capacity of 8.2×10^8 m³ could be formed, and the flood would reach Danba city after passing the intersection of rivers and flowing up the Dajinchuan River basin without engineering measures, which would be devastating to downstream areas.

DATA AVAILABILITY STATEMENT

The original contributions presented in the study are included in the article/Supplementary Material, further inquiries can be directed to the corresponding author.

AUTHOR CONTRIBUTIONS

LN: Formal analysis, Writing—Original Draft; KH: Supervision, Conceptualization, Funding acquisition; ZW: Writing—Review and Editing; HL: Data Curation; HQ: Data Curation; XZ: Visualization; SL: Funding acquisition.

FUNDING

This study was supported by the National Key R and D Program of China (2020YFD1100701), the National Natural Science Foundation of China (41790434), the National Key R and D Program of China (2018YFC1505205), the Research on Intelligent Monitoring and Early Warning Technology of Debris Flow on the Sichuan-Tibet Railway (K2019G006), and the National Key Research and Development Program of China (2018YFC1505503).

REFERENCES

Abidin, R. Z., Sulaiman, M. S., and Yusoff, N. (2017). Erosion Risk Assessment: a Case Study of the Langat River Bank in Malaysia. *Int. Soil Water Conservation Res.* 5, 26–35. doi:10.1016/j.iswcr.2017.01.002

Bouwer, L. M., Papyrakis, E., Poussin, J., Pfurtscheller, C., and Thieken, A. H. 2014. The Costing of Measures for Natural Hazard Mitigation in Europe. Natural Hazards Review 15.

Carpignano, A., Golia, E., Di Mauro, C., Bouchon, S., and Nordvik, J. P. (2009). A Methodological Approach for the Definition of Multi-risk Maps at Regional Level: First Application. *J. Risk Res.* 12, 513–534. doi:10.1080/13669870903050269

Chai, H. J., Liu, H. C., and Zhang, Y. Y. (1995). Catalogue of Landslide and River Blocking Events in China. *Geol. hazards Environ. Prot.* 006, 1–9.

Chen, L., Westen, C. J. V., Hussin, H., Ciurean, R. L., Turkington, T., Chavarro-Rincon, D., et al. (2016). Integrating Expert Opinion with Modelling for Quantitative Multi-hazard Risk Assessment in the Eastern Italian Alps. *Geomorphology* 273, 150–167. doi:10.1016/j.geomorph.2016.07.041

Chen, X. Q., Cui, P., Li, Y., and Zhao, W. Y. (2011). Emergency Response to the Tangjiashan Landslide-Dammed lake Resulting from the 2008 Wenchuan Earthquake, China. *Landslides* 8, 91–98. doi:10.1007/s10346-010-0236-6

Chen, Z. Y., Ma, L., Yu, S., Chen, S., Zhou, X., and Sun, P. (2015). Back Analysis of the Draining Process of the Tangjiashan Barrier lake. *J. Hydraulic Eng.* 141, 05014011.1–05014011.14. doi:10.1061/(ASCE)HY.1943-7900.0000965

Costa, J. E., and Schuster, R. L. (1988). The Formation and Failure of Natural Dams. *Geol. Soc. America Bull.* 100, 1054–1068. doi:10.1130/0016-7606(1988)100<1054:tfafon>2.3.co;2

Cui, P., Chen, X. Q., Zhu, Y. Y., Su, F. H., Wei, F. Q., Han, Y. S., et al. (2011). The Wenchuan Earthquake (May 12, 2008), Sichuan Province, China, and Resulting Geohazards. *Nat. Hazards* 56, 19–36. doi:10.1007/s11069-009-9392-1

Cui, P., Su, F., Zou, Q., Chen, N., and Zhang, Y. (2015). Risk Assessment and Disaster Reduction Strategies for Mountainous and Meteorological Hazards in Tibetan Plateau. *Chin. Sci. Bull.* 60, 3067–3077. doi:10.1360/n972015-00849

Davies, T. R. (1997). "Using Hydroscience and Hydrotechnical Engineering to Reduce Debris Flow Hazards," in *First International Conference On Debris Flow Hazards Mitigation* (San Francisco: ASCE), 787–810.

Delmonaco, G., Margottini, C., and Spizzino, D. (2006). Report on New Methodology for Multi-Risk Assesment and the Harmonisation for Different Natural Risk Maps, Armonia Project. Rome, Italy: ASCE.

Deng, M., Chen, N., and Liu, M. (2017). Meteorological Factors Driving Glacial till Variation and the Associated Periglacial Debris Flows in Tianmo Valley, South-Eastern Tibetan Plateau. *Nat. Hazards Earth Syst. Sci.* 17, 345–356. doi:10.5194/nhess-17-345-2017

Fan, X., Tang, C. X., Van Westen, C. J., and Alkema, D. (2012). Simulating Dam-Breach Flood Scenarios of the Tangjiashan Landslide Dam Induced by the Wenchuan Earthquake. *Nat. Hazards Earth Syst. Sci.* 12, 3031–3044. doi:10.5194/nhess-12-3031-2012

Fan, X., Yang, F., Siva Subramanian, S., Xu, Q., Feng, Z., Mavrouli, O., et al. (2020). Prediction of a Multi-hazard Chain by an Integrated Numerical Simulation Approach: the Baige Landslide, Jinsha River, China. *Landslides* 17, 147–164. doi:10.1007/s10346-019-01313-5

Ge, Y.-g., Cui, P., Su, F.-h., Zhang, J.-q., and Chen, X.-z. (2014). Case History of the Disastrous Debris Flows of Tianmo Watershed in Bomi County, Tibet, China: Some Mitigation Suggestions. *J. Mt. Sci.* 11, 1253–1265. doi:10.1007/s11629-014-2579-2

Gilbuena, R., Jr, Kawamura, A., Medina, R., Amaguchi, H., Nakagawa, N., and Bui, D. D. (2013). Environmental Impact Assessment of Structural Flood Mitigation Measures by a Rapid Impact Assessment Matrix (RIAM) Technique: A Case Study in Metro Manila, Philippines. *Sci. Total Environ.* 456-457, 137–147. doi:10.1016/j.scitotenv.2013.03.063

Hermanns, R. L., Niedermann, S., Ivy-Ochs, S., and Kubik, P. W. (2004). Rock Avalanching into a Landslide-Dammed lake Causing Multiple Dam Failure in Las Conchas valley (NW Argentina)—evidence from Surface Exposure Dating and Stratigraphic Analyses. *Landslides* 1, 113–122. doi:10.1007/s10346-004-0013-5

Hu, K., Zhang, X., and Luo, H. (2020). Investigation of the "6.17" Debris Flow Chain at the Meilong Catchment of Danba County, China. *Mountain Res.* 38 (06), 945–951. doi:10.16089/j.cnki.1008-2786.000570

Hu, K., Zhang, X., Tang, J., and Liu, W. (2018). "Potential Danger of Dammed Lakes Induced by the 2017 Ms6. 9 Mifflin Earthquake in the Tsangpo Gorge," in *5th International Conference Debris Flows: Disasters, Risk, Forecast, Protection* (Tbilisi: Publishing House "Universal"), 97–104.

Hu, K., Zhang, X., You, Y., Hu, X., Liu, W., and Li, Y. (2019a). Landslides and Dammed Lakes Triggered by the 2017 Ms6.9 Milin Earthquake in the Tsangpo Gorge. *Landslides* 16, 993–1001. doi:10.1007/s10346-019-01168-w

Hu, X., Hu, K., Tang, J., You, Y., and Wu, C. (2019b). Assessment of Debris-Flow Potential Dangers in the Jiuzhaigou Valley Following the August 8, 2017, Jiuzhaigou Earthquake, Western China. *Eng. Geology.* 256, 57–66. doi:10.1016/j.enggeo.2019.05.004

Kappes, M. S., Keiler, M., von Elverfeldt, K., and Glade, T. (2012). Challenges of Analyzing Multi-hazard Risk: a Review. *Nat. Hazards* 64, 1925–1958. doi:10.1007/s11069-012-0294-2

Korup, O., and Clague, J. J. (2009). Natural Hazards, Extreme Events, and Mountain Topography. *Quat. Sci. Rev.* 28, 977–990. doi:10.1016/j.quascirev.2009.02.021

Liu, W., and He, S. (2018). Dynamic Simulation of a Mountain Disaster Chain: Landslides, Barrier Lakes, and Outburst Floods. *Nat. Hazards* 90, 757–775. doi:10.1007/s11069-017-3073-2

Luo, H., Zhang, L., Wang, H., and He, J. (2020). Multi-hazard Vulnerability of Buildings to Debris Flows. *Eng. Geology.* 279, 105859. doi:10.1016/j.enggeo.2020.105859

Ma, C., and Kaiheng, H. (2013). Processes and Characteristics of Debris Flow Induced by Maoqiaozi Landslide in Wenchuan Earthquake Stricken Area. *J. Earth Sci. Environ.* 35, 98–103. doi:10.3969/j.issn.1672-6561.2013.04.011

Mechler, R. (2016). Reviewing Estimates of the Economic Efficiency of Disaster Risk Management: Opportunities and Limitations of Using Risk-Based Cost-Benefit Analysis. *Nat. Hazards* 81, 2121–2147. doi:10.1007/s11069-016-2170-y

Ouyang, C. J., He, S. M., Xu, Q., Luo, Y., and Zhang, W. C. (2013). A MacCormack-TVD Finite Difference Method to Simulate the Mass Flow in Mountainous Terrain with Variable Computational Domain. *Comput. Geosciences* 52, 1–10. doi:10.1016/j.cageo.2012.08.024

Papathoma-Köhle, M., Kappes, M., Keiler, M., and Glade, T. (2011). Physical Vulnerability Assessment for alpine Hazards: State of the Art and Future Needs. *Nat. Hazards* 58, 645–680. doi:10.1007/s11069-010-9632-4

Rahardjo, H., Li, X. W., Toll, D. G., and Leong, E. C. (2001). The Effect of Antecedent Rainfall on Slope Stability. *Geotech. Geol. Eng.* 19 (3-4), 371–399. doi:10.1023/a:1013129725263

Reneau, S. L., and Dethier, D. P. (1996). Late Pleistocene Landslide-Dammed Lakes along the Rio Grande, White Rock Canyon, New Mexico. *Geol. Soc. America Bull.* 108, 1492–1507. doi:10.1130/0016-7606(1996)108<1492:lpldla>2.3.co;2

Shi, Z. M., Xiong, X., Peng, M., Zhang, L. M., Xiong, Y. F., Chen, H. X., et al. (2017). Risk Assessment and Mitigation for the Hongshiyan Landslide Dam Triggered by the 2014 Ludian Earthquake in Yunnan, China. *Landslides* 14, 269–285. doi:10.1007/s10346-016-0699-1

Sun, Y., and Li, J. (2019). Analysis on the Formation Conditions and Basic Characteristics of the Debris Flow in Meilonggou in Banshanmen Township. *Danba County Sci. Technology Innovation Bull.* 16, 115–116.

van Westen, C., Kappes, M. S., Luna, B. Q., Frigerio, S., Glade, T., and Malet, J.-P. (2014). "Medium-Scale Multi-hazard Risk Assessment of Gravitational Processes," in *Mountain Risks: From Prediction to Management and Governance. Advances in Natural and Technological Hazards Research*. Editors T. Van Asch, J. Corominas, S. Greiving, J. P. Malet, and S. Sterlacchini (Dordrecht: Springer), Vol. 34, 201–231. doi:10.1007/978-94-007-6769-0_7

Worni, R., Huggel, C., Clague, J. J., Schaub, Y., and Stoffel, M. (2014). Coupling Glacial lake Impact, Dam Breach, and Flood Processes: A Modeling Perspective. *Geomorphology* 224, 161–176. doi:10.1016/j.geomorph.2014.06.031

Xu, M., Wang, Z., Qi, L., Liu, L., and Zhang, K. (2012). Disaster Chains Initiated by the Wenchuan Earthquake. *Environ. Earth Sci.* 65, 975–985. doi:10.1007/s12665-011-0905-3

Xu, M., W.Zhaoyin, Y., Wenjing, S., and Xuzhao, W. (2010). Chain of Secondary Mountain Disaster Caused by Wenchuan Earthquake - Take Huoshigou as an Example. *J. Tsinghua Univ. - Nat. Sci. Edition* 2010, 20–23.

Yao, T., lijuan, W., and Juan, Z. (2020). Application of Remote Sensing Technology in Emergency rescue and rescue Decision Making in the "June 17" Dam Dadu River Debris Flow Disaster Chain Disaster Area. *Geol. Surv. China* 7, 114–122. doi:10.19388/j.zgdzdc.2020.05.13

Yu, F. (2018). *Research on Development Characteristics, Cause Analysis and Prevention of Debris Flow Geological Disaster in Danba County, 24–27*. Chengdu, China: Southwest Jiaotong University.

Zhang, L. M., He, J., and Xiao, T. (2020). "Engineering Risk Mitigation for Landslide Hazard Chains: The Baige Landslides on the Jinsha River in 2018," in *Understanding and Reducing Landslide Disaster Risk. WLF 2020. ICL Contribution to Landslide Disaster Risk Reduction*. Editors B. Tiwari, K. Sassa, P. T. Bobrowsky, and K. Takara (Cham: Springer), 109–120. doi:10.1007/978-3-030-60706-7_6.

Zhao, B., Zhang, H., Hongjian, L., Li, W., Su, L., He, W., et al. (2021). Emergency Response to the Reactivated Aniangzhai Landslide Resulting from a Rainstorm-Triggered Debris Flow, Sichuan Province, China. *Landslides* 18, 1115–1130. doi:10.1007/s10346-020-01612-2

Conflict of Interest: The authors declare that the research was conducted in the absence of any commercial or financial relationships that could be construed as a potential conflict of interest.

Publisher's Note: All claims expressed in this article are solely those of the authors and do not necessarily represent those of their affiliated organizations, or those of the publisher, the editors, and the reviewers. Any product that may be evaluated in this article, or claim that may be made by its manufacturer, is not guaranteed or endorsed by the publisher.